Formation of Regular Magnetic Domains on Spontaneously Nanostructured Cobalt Filaments

By *Xiao-Ping Huang, Zi-Liang Shi, Mu Wang,* Makoto Konoto, Hao-Shen Zhou, Guo-Bin Ma, Di Wu, Ruwen Peng,* and *Nai-Ben Ming*

Magnetic domains are spontaneous structures in ferromagnetic materials that form the basis for modern data storage and information access. Formation of magnetic domains depends on the balance of exchange energy, magnetostatic energy, and anisotropic energy, following the principle that the gain in magnetostatic energy due to a reduced demagnetization field should be larger than the energy cost of creating the domain walls.[1] As spintronics is being developed, great efforts have been devoted to manipulate domain structures in rectangles with geometrical constrictions,[2–5] notched rings,[6–9] necked wires and stripes[10–15] on the micrometer and nanometer scales with the aim of finding new principles of information access techniques and of promoting the development of magneto-electronics. It has been shown that when the lateral dimensions are reduced, the geometry, rather than the material parameters, determines the type of domain wall and the spin structure, and hence controls the magnetic property.[16] Instead of applying an external magnetic field, it has recently been discovered that a spin-polarized electric current may move the magnetic domain walls, which holds the prospect of achieving non-volatile memory devices with high performance and reliability.[17–19] It is expected that the static and dynamic behaviors of domain walls on nanowires will determine the properties of these devices. For this purpose, introducing periodically ordered magnetic domain structures is essential, which is normally realized by state-of-the-art electron-beam lithography or focused ion beam techniques.[17–19] These fabrication processes are precise and accurately controlled, yet cost and time are factors that might hinder their wide application.

Here we demonstrate a unique electrodeposition approach which allows the spontaneous self-organization of periodically corrugated nanostructures on the cobalt filaments. The periodicity of the corrugations can be tuned from a few tens to hundreds of nanometers. Experiments show that the geometry of the filaments determines the domain wall structures. When the spatial periodicity is short, a single domain state accompanied by anti-parallel magnetization is stable. When the spatial periodicity is large, vortex domains are formed instead. The formation mechanism and evolution principle of the magnetic domains on the filaments are discussed.

An aqueous electrolyte solution of $CoSO_4$ with an initial concentration of 0.02 M was used for electrodeposition, where two straight, parallel cobalt electrodes were sandwiched by two glass plates as substrates. In order to suppress convective disturbances during the electrodeposition process,[20] we solidified the electrolyte layer from beneath. When equilibrium was eventually achieved, an ultrathin film of electrolyte solution existed between the icy electrolyte and the glass substrate because of the partitioning effect during solidification, which is where our electrodeposits were grown.[21,22] The thickness of this trapped electrolyte layer varied depending on the temperature and the initial concentration of the electrolyte. At $-4\,^{\circ}C$ and an initial concentration of 0.02 M of the electrolyte, the thickness of this layer was on the order of 200 nm. Our experiments were controlled galvanostatically. When cobalt electrodeposition started, branched cobalt filaments initiated from the cathode, developed on the glass substrate and extended towards the anode. In galvanostatic mode, the applied electric current remained constant, yet the voltage across the electrodes oscillated spontaneously,[21,22] and led to the periodic corrugations on the filaments.

A typical scanning electron microscopy (SEM) image of the cobalt filaments is shown in Figure 1a. Periodically corrugated structures can be clearly identified on the filaments, and the periodic structures on all the branches are synchronized. This means that the corrugations on the neighboring filaments are all correlated, which can be very easily recognized at the branching site, as marked by the dashed circles in Figure 1b. Atomic force microscopy (AFM) showed that the thickness of the filaments is about 50 nm, and the depth of the ditches on the filaments is of the order of 20 nm. The filaments are polycrystalline consisting mainly of cobalt and a small amount of cobalt oxide. The transmission electron microscopy (TEM) (Fig. 1c) and Energy dispersive X-ray (EDX) analysis shown in Figure 1c confirm that the concentration of oxygen vs. cobalt at the ditches between the

[*] Prof. M. Wang, Dr. X. P. Huang,[+] Dr. Z. L. Shi, Dr. G. B. Ma, Prof. D. Wu, Prof. R. W. Peng, Prof. N. B. Ming
National Laboratory of Solid State Microstructures, Nanjing University
Nanjing 210093 (P.R. China)
E-mail: muwang@nju.edu.cn
Dr. M. Konoto
Nanoelectronics Research Institute, National Institute of Advanced Industrial Science and Technology (AIST)
Higashi 1-1-1, Tsukuba, 305-8562 (Japan)
Dr. H. S. Zhou
Energy Technology Research Institute, National Institute of Advanced Industrial Science and Technology (AIST)
Umezono 1-1-1, Tsukuba, 305-8568 (Japan)
[+] Present address: School of Physical Electronics, University of Electronic Science and Technology of China, Chengdu 610054 (P.R. China)

DOI: 10.1002/adma.200904066

neighboring corrugations is higher than in the other regions, which is consistent with our previous observations of non-magnetic copper electrodeposition.[21,22] By spontaneously synchronized, alternating electro- deposition of cobalt and cobalt oxides, nanostructured filaments were generated. The spatial periodicity on the filaments could be tuned by changing the electric current, temperature, or initial electrolyte concentration.

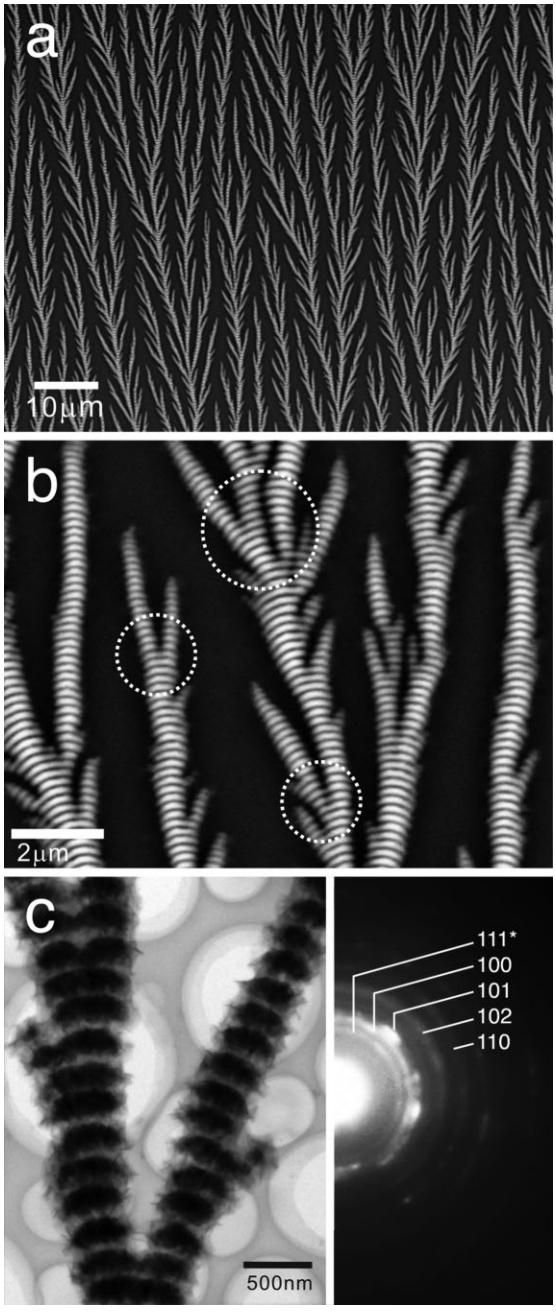

Figure 1. a) SEM image of the cobalt filament array. b) SEM image of the cobalt filaments at higher magnification. The periodic corrugations on the filaments can be clearly identified. The correlation of corrugations on neighboring branches can be easily recognized especially in the branching region as marked by the circles. c) TEM image of a cobalt filament (left) and its diffraction pattern (right). The strongest diffraction comes from cobalt (101). Weak diffraction of CoO(111) can also be identified (the ring indexed with a star). EDX analysis shows that in the junction region the concentration of oxide is much higher.

Magnetic force microscopy (MFM) images indicated that the configuration of the magnetic domains on the filaments depends on the geometrical periodicity. Figure 2 shows the MFM images of as-grown cobalt filaments with different spatial periodicity measured at room temperature. For a filament with a certain width, when the spatial periodicity on the filament becomes comparable to the filament width, as marked by the boxes in Figure 2a and b, each geometrical block on the filament corresponds to two reversely positioned black–white contrast pairs in the MFM image, which are induced by the vortex magnetization in the block.[23,24] Such a relation can be clearly seen in Figure 2c, which shows the topography and the MFM images of the boxed regions in Figure 2a and b. On the right-hand side of Figure 2c, a drawing was made to function as a guide to the eye to show how two reversely oriented domains (in fact here it is a vortex domain) are arranged in a spatial period on the filament. By increasing the electric current of the electrodeposition, the oscillation frequency is increased and the spatial periodicity on filaments is effectively decreased. When the spatial periodicity of the corrugations becomes much shorter than the width of the filament, as shown in Figure 2d and e, each corrugation corresponds to a single domain, and the neighboring domains exhibit anti-parallel ordering. Figure 2f shows the boxed regions in Figure 2d and e. Again on the right-hand side of Figure 2f a drawing illustrates the domain orientation and the arrows show the local orientation of magnetization. It should be noted that each corrugation in topography corresponds to black–white contrasted pair, and the neighboring pairs are reversed in polarity. This means that the magnetization is transversely perpendicular to the filament. Therefore, for filaments with a certain width, the type of magnetic domains on the filaments can be tuned by the spatial periodicity of the corrugations on the filaments.

The dependence of magnetic domain and spatial periodicity on the as-grown filaments was further verified by spin-polarized scanning electron microscopy (spin-SEM).[23] With this technique, the real-space distribution of magnetization can be visualized by detecting the spin polarization of the secondary electrons, which reflects local magnetization at the emission site. The magnetization directions in the corrugated structures can be quantitatively analyzed on the nanoscale. Figure 3a illustrates the topography of the electrodeposits with periodic corrugations. It is noteworthy that one section of the corrugation in the picture is much larger than the neighboring ones because of fluctuations in the growth conditions, and thus some trapezoidal microstructures, one of which has been marked by box A, are formed in this section. Figure 3b shows the local magnetization directions of the region shown in Figure 3a, as represented by the color wheel on the right-hand side of the image. In the trapezoidal region (the area marked as box A, for example), we can clearly identify a magnetic vortex structure composed of four domains, as schematically shown in Figure 3c. This type of multidomain structure is often developed in microstructured rectangular magnets and quite stable because of the magnetic flux closure within the domains.[24]

In the regions with shorter spatial periodicity (around 200 nm), however, the single-domain state is more stable, forming an anti-ferromagnetic-like magnetization arrangement, as shown in the area marked by box B in Figure 3a and b, and also schematically

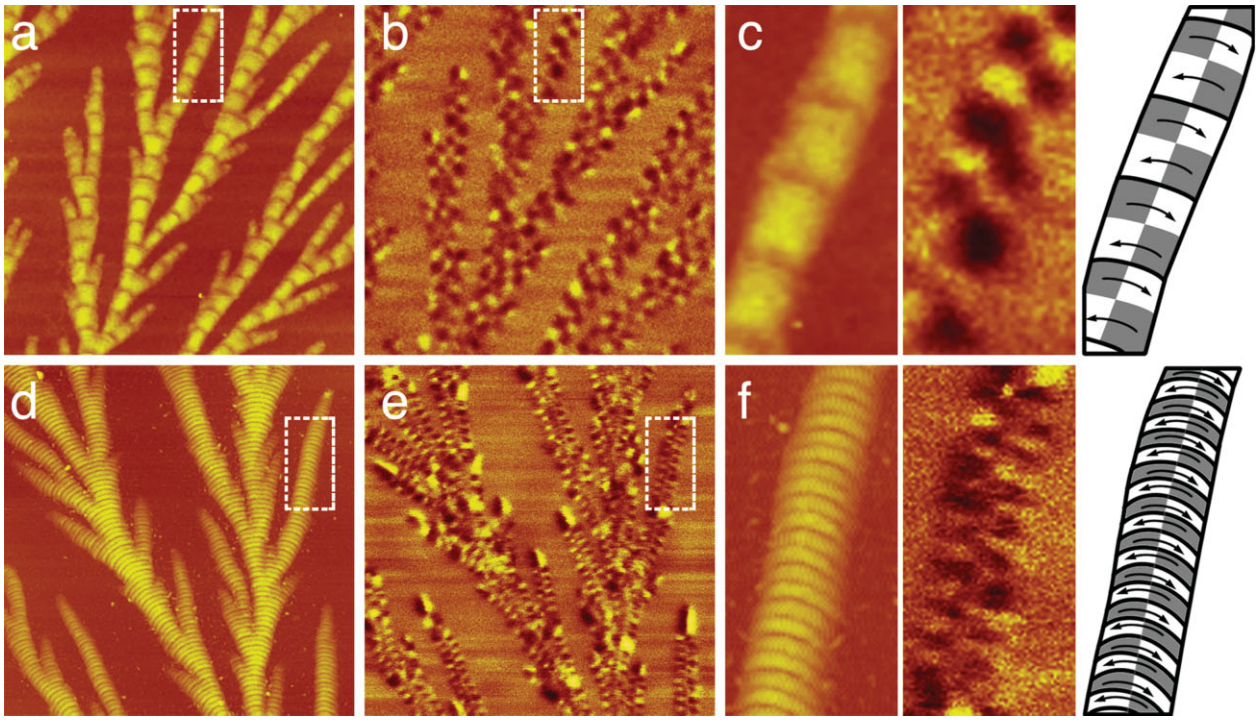

Figure 2. MFM images showing the topography of the filaments and magnetic domains on them. a,b) Topography (a) and magnetic domains (b) for filaments where the periodicity of the corrugations is comparable to the filament width. c) Details of the boxed regions in (a) and (b). d,e) Topography (d) and magnetic domains (e) of nanostructured filaments where the periodicity of the corrugations on the filament is much smaller than the filament width. f) Details of the boxed regions in (d) and (e). The drawings on the far right-hand side serve as a guide to the eye to illustrate the local magnetization directions on the filament.

shown in Figure 3d. The magnetization is oriented anti-parallel to the adjacent ones in order to efficiently reduce the magnetostatic energy caused by stray magnetic fields from the side surface of the filament. Although the perfectly anti-parallel arrangement is relatively stable, we still observed that in a number of regions the modulations become locally disordered because of fluctuations. It has been established that if the size of a magnetic particle becomes smaller than a critical size, the single-domain state becomes more stable.[25] The observation shown here manifests that in our system the critical size is greater than 200 nm, and our current electrodeposition technique has been able to fabricate sufficiently small corrugations to stabilize the single-domain state.

MFM images also indicated that a long, single magnetic domain also exists at the end of each electrodeposited filament, as shown in Figure 4a and b. The single domain at the tip of the filament extends across several spatial corrugations, which is characterized by the elongated dark-bright contrast, as marked by the circles. Whereas on the main part of the filament, either anti-parallel or vortex domains are observed. On the right-hand side of Figure 4b, a drawing illustrates the magnetization at the tip region. Comparing Figure 4 with Figures 2 and 3, we may infer that in this scenario the magnetization is in-plane and perpendicular to the filament. In fact, Figure 4a and b can be considered as a snapshot of a certain moment in the filament's growth, which becomes particularly helpful in understanding the formation and the evolution of magnetic domains on the filament. To check the stability of the domain structures, we applied an in-plane alternative magnetic field of 1.0 T to demagnetize the filaments. The orientation of the magnetic field was almost in parallel with the filaments. After demagnetization, exactly the same area was rescanned by MFM, as illustrated in Figure 4c and d. As indicated by the circles, after demagnetization, the tip regions of the filaments become multidomained, whereas the multidomain features on the main parts of the filaments remain. Once again a drawing is shown on the right-hand side of Figure 4d to schematically illustrate the local magnetization in the tip region. We expect that demagnetization induces a lower energy state in the filaments. Hence, the initial single magnetic domain on the filament tip decomposes to the more stable multidomain structure.

Figure 4 implies that the periodic magnetic domains on the filaments might all originate from a giant single domain at the tip of the filament that after some time evolves into multidomains in order to reduce the magnetostatic energy. Does this mean that in this far-from-equilibrium growth, the system does not have enough time to relax to a state with sufficiently low energy, so a single-domain region is temporarily preserved at the tip of the filaments? To verify the relationship between the type of magnetic domains and the driving force of filament growth, we tuned the electric current during the electrodeposition process and studied the corresponding changes in the magnetic domains of the cobalt filaments. Figure 5a shows the topography of the cobalt filaments before and after a sudden increase in electric current during

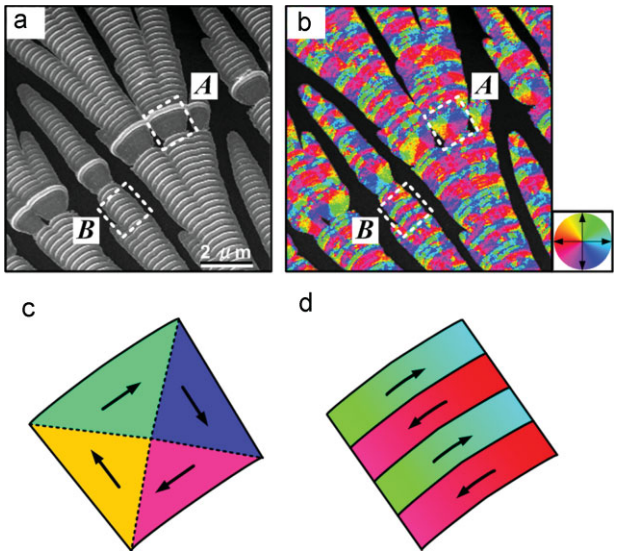

Figure 3. Spin-polarized SEM images of the cobalt filaments in the as-grown state. a) Topographic image of the filaments. A section of the corrugation, including boxed region A, is much wider than the neighboring ones because of fluctuations in the growth conditions. b) Real-space distribution of local magnetization directions in the corresponding region. The color wheel represents the magnetization direction. In boxed region A, the spatial periodicity of the corrugation is rather large, so a typical flux-closed multi-domain structure illustrated in (c), a so-called magnetic vortex, is formed. In boxed region B, however, the spatial periodicity is shorter than a threshold value and single domains with alternate magnetization become stable, as schematically shown in (d) (see text). The arrows in (c) and (d) represent deduced magnetization directions.

electrodeposition. A boundary can be identified where the current was changed, as indicated along the direction of the black arrow. At higher electric currents the electrodeposits develop faster, and the growth is further away from equilibrium. Figure 5b shows the corresponding MFM image. It can be seen that in the case of high electrodeposition current, most of the magnetic domains are single domains extending to a length covering many spatial corrugations. The neighboring single domains on the filament have alternate polarizations because of long-range magnetostatic interactions.

The periodic corrugations on the cobalt filaments play a key role in stabilizing the magnetic domains.[17–19] As we demonstrated previously,[22] the periodicity of the corrugations on metallic filaments can be tuned by changing the electric current/voltage during electrodeposition, and the spatial periodicity is homogeneous. Therefore, our experiment demonstrates a convenient way for introducing regularly spaced magnetic domains on magnetic metal filaments.

Electron diffraction analysis of the filaments indicated that our cobalt filaments are polycrystalline, and the magnetocrystalline anisotropy of the crystallites is negligible. Hence the shape anisotropy of the nanostructured filaments becomes more important. The typical width of the filaments is of the order of 500–800 nm, whereas the typical length of the filament without sidebranching is of the order of several micrometers. Therefore, if there were no additional structures on the filaments, the magnetic polarization of each filament should be along the longitudinal direction. However, because of the corrugations on the filament the situation is changed. The typical spatial periodicity of the corrugations is of the order of 100 nm, which is much smaller than the width of the filament. Microscopically the magnetization follows the local anisotropy. The compromise of the shape anisotropy on these two levels eventually determines the domain pattern. As illustrated in Figure 2, depending on spatial periodicity, the magnetic domain will possess either a vortex pattern or an anti-parallel single-domain pattern in the direction perpendicular to the filament.

It has recently been suggested that by introducing a spin-polarized electric current pulse to a ferromagnetic stripe, a train of magnetic domain walls can be simultaneously moved at the same speed over a fixed reading (or writing) head for sequential reading (or writing).[17,18] A reverse current can move the domain walls in the opposite direction for resetting.[26] This mimics the fast passing of bits in front of the head in hard-disk recording, with the benefit of not needing any mechanical moving parts in the process. Instead of applying complicated photolithography techniques, our experiment demonstrates an easy, self-organized electrochemical way to fabricate a ferromagnetic filament array with periodic corrugations on the surface.

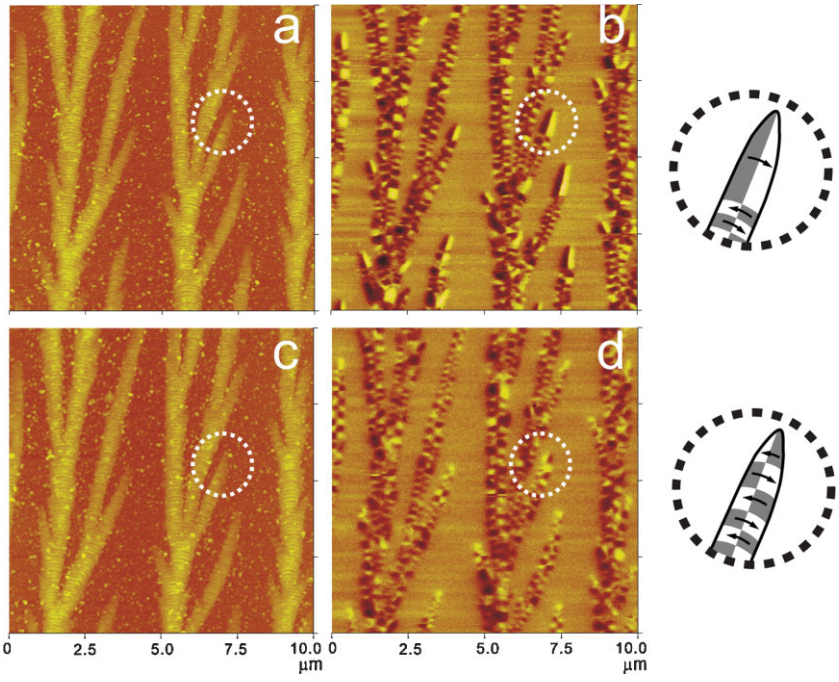

Figure 4. MFM images of the microstructured cobalt filaments before (a,b) and after (c,d) demagnetization. Before demagnetization, a large single domain exists on the tip region of each filament, as marked by the circle in (b). After demagnetization, the single domain on the filament tip evolves into multidomains, as indicated in (d). The drawings on the right-hand side of (b) and (d) serve as a guide to the eye to illustrate the local magnetization on the tip of the filament before and after demagnetization, respectively.

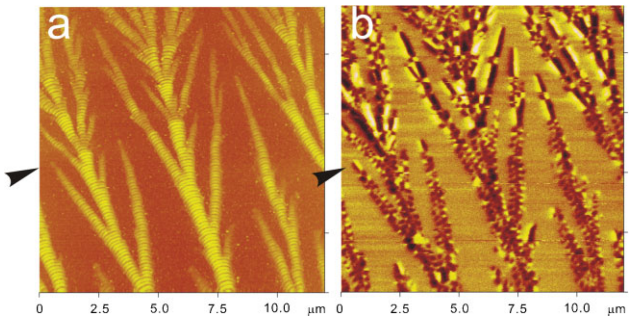

Figure 5. MFM image of the filament to show the dependence of the magnetic domains and the driving force of filament growth. A boundary can be identified in (a), along the direction of the black arrow, below which the filaments grew with lower electric current; across the boundary, the electric current for electrodeposition increased suddenly. This means that above the boundary, the driving force for filament growth was higher. Consequently, the magnetic domains above the boundary are large single domains, which extend several spatial corrugations and are in clear contrast to those below the boundary.

These corrugated structures are important to stabilize the domain distribution. Although we have not yet concluded experiments of electric-current-driven domain movement, our novel fabrication method that allows the type of magnetic domains on the filaments to be selected will attract the attention of those exploring different new materials (and structures) for data storage and magnetic logic devices.

To summarize, we demonstrate in this communication the self-organization of magnetic domains on cobalt filaments by a unique electrodeposition method. MFM and spin-SEM imaging indicate that the type of magnetic domains depends on the spatial periodicity of the corrugations on the filaments: The anti-parallel arranged single domains appear when the periodicity of corrugation is short; whereas vortex domain structures appear when the periodicity is longer. Large single domains across several spatial corrugations appear either on the tip of the filament, or when the driving force of filament growth is suddenly increased. Demagnetization changes these giant single domains into multidomains, confirming that the domain formation is ultimately an energy-minimizing process. Our experiments demonstrate a new approach to fabricate periodic magnetic domain structures, which might have potential application in spintronics, and are helpful in understanding the formation and evolution of microscopic magnetic domains.

Experimental

Self-Organized Growth of Cobalt Filaments: An aqueous electrolyte of $CoSO_4$ for electrodeposition was prepared by dissolving $CoSO_4$ (analytical pure, 99.5%) with de-ionized ultrapure water (Millipore, electric resistivity 18.2 MΩ · cm), and the initial concentration was 0.02 M. Straight parallel electrodes were made of pure cobalt wire (99.995% pure, ø 0.1 mm, Alfa Aesar), and were sandwiched by two glass plates (substrates). The electrodes were 10 mm apart. In order to suppress convective disturbances during the electrodeposition,[20] we applied a unique method by solidifying the electrolyte from beneath and to form an ultrathin film of electrolyte solution between the icy electrolyte and the glass substrate.[21,22] The ultrathin film of electrolyte, which was generated because of the partitioning effect in solidification, had a variable thickness depending on the temperature of the electrodeposition cell. At −4 °C and for a 0.02 M electrolyte solution, the thickness of this trapped film was of the order of 200 nm. In our experiments galvanostatic control was used. When cobalt electrodeposition started, branched cobalt filaments initiated from the cathode developed on the glass substrate and extended towards the anode. During this galvanostatic electrodeposition, the voltage across the electrodes oscillated spontaneously [21,22] and led to the periodic corrugations on the filaments.

Structural and Magnetic Characterization: The cobalt arrays were observed with a field-emission scanning electron microscope (LEO 1530VP) in the InLens mode. The structure of cobalt filaments was characterized by a transmission electron microscope (JEOL 4000EX). An atomic force microscope (Digital Instruments, Nanoscope IIIa) was used in the MFM mode to measure the topography of the filaments and magnetic domains on the filaments. The dependence of the magnetic domain type and spatial periodicity on the cobalt filaments was further verified with a spin-polarized scanning electron microscope, and the instrument details have been provided before [23].

Acknowledgements

The financial supports from the Ministry of Science and Technology of China (2006CB921804 and 2010CB630705), NSF of China (10874068 and 10625417), and Jiangsu Province (BK2008012) are acknowledged.

Received: November 27, 2009
Published online: April 6, 2010

[1] A. Aharoni, *Introduction to the Theory of Ferromagnetism*, Oxford University Press, New York, NJ **2000**.
[2] S. Blomeier, B. Hillebrands, B. Reuscher, A. Brodyanski, M. Kopnarski, R. L. Stamps, *Phys. Rev. B* **2008**, *77*, 094405.
[3] Y. Takagaki, K. H. Ploog, *Phys. Rev. B* **2005**, *71*, 184439.
[4] J. L. Costa-Krämer, R. Alvarez-Sanchez, A. Bengoechea, F. Torres, P. Garcia-Mochales, F. Briones, *Phys. Rev. B* **2005**, *71*, 104420.
[5] M. Bolte, R. Eiselt, G. Meier, D. H. Kim, P. Fischer, *J. Appl. Phys.* **2006**, *99*, 08H301.
[6] V. Novosad, K. Y. Guslienko, H. Shima, Y. Otani, S. G. Kim, K. Fukamichi, N. Kikuchi, O. Kitakami, Y. Shimada, *Phys. Rev. B* **2002**, *65*, 060402.
[7] K. Y. Guslienko, V. Novosad, Y. Otani, H. Shima, K. Fukamichi, *Appl. Phys. Lett.* **2001**, *78*, 3848.
[8] T. Shinjo, T. Okuno, R. Hassdorf, K. Shigeto, T. Ono, *Science* **2000**, *289*, 930.
[9] Y. B. Xu, A. Hirohata, L. Lopez-Diaz, H. T. Leung, M. Tselepi, S. M. Gardiner, W. Y. Lee, J. A. C. Bland, F. Rousseaux, E. Cambril, H. Launois, *J. Appl. Phys.* **2000**, *87*, 7019.
[10] D. Backes, C. Schieback, M. Klaui, F. Junginger, H. Ehrke, P. Nielaba, U. Rudiger, L. J. Heyderman, C. S. Chen, T. Kasama, R. E. Dunin-Borkowski, C. A. F. Vaz, J. A. C. Bland, *Appl. Phys. Lett.* **2007**, *91*, 112502.
[11] R. P. Cowburn, D. K. Koltsov, A. O. Adeyeye, M. E. Welland, D. M. Tricker, *Phys. Rev. Lett.* **1999**, *83*, 1042.
[12] L. K. Verma, V. Ng, *J. Appl. Phys.* **2008**, *103*, 053902.
[13] U. Ruediger, J. Yu, S. Zhang, A. D. Kent, S. S. P. Parkin, *Phys. Rev. Lett.* **1998**, *80*, 5639.
[14] T. R. Gao, L. F. Yin, C. S. Tian, M. Lu, H. Sang, S. M. Zhou, *J. Magn. Magn. Mater.* **2006**, *300*, 471.
[15] T. Schmitte, K. Theis-Brohl, V. Leiner, H. Zabel, S. Kirsch, A. Carl, *J. Phys.: Condens. Matter* **2002**, *14*, 7525.
[16] M. H. Pan, H. Liu, J. Z. Wang, J. F. Jia, Q. K. Xue, J. L. Li, S. Qin, U. M. Mirsaidov, X. R. Wang, J. T. Markert, Z. Y. Zhang, C. K. Shih, *Nano Lett.* **2005**, *5*, 87.
[17] S. S. P. Parkin, M. Hayashi, L. Thomas, *Science* **2008**, *320*, 190.
[18] M. Hayashi, L. Thomas, R. Moriya, C. Rettner, S. S. P. Parkin, *Science* **2008**, *320*, 209.

[19] D. A. Allwood, G. Xiong, C. C. Faulkner, D. Atkinson, D. Petit, R. P. Cowburn, *Science* **2005**, *309*, 1688.
[20] M. Wang, W. J. P. van Enckevort, N.-B. Ming, P. Bennema, *Nature* **1994**, *367*, 438.
[21] M. Wang, S. Zhong, X. B. Yin, J. M. Zhu, R. W. Peng, Y. Wang, K. Q. Zhang, N. B. Ming, *Phys. Rev. Lett.* **2001**, *86*, 3827.
[22] S. Zhong, Y. Wang, M. Wang, M. Z. Zhang, X. B. Yin, R. W. Peng, N. B. Ming, *Phys. Rev. E* **2003**, *67*, 061601.
[23] M. Konoto, T. Kohashi, K. Koike, T. Arima, Y. Kaneko, T. Kimura, Y. Tokura, *Phys. Rev. Lett.* **2004**, *93*, 107201.
[24] M. Konoto, T. Yamada, K. Koike, H. Akoh, T. Arima, Y. Tokura, *J. Appl. Phys.* **2008**, *103*, 023904.
[25] C. Kittel, *Phys. Rev.* **1946**, *70*, 965.
[26] The introductory information can be found on the IBM Research SpinAps website: www.almaden.ibm.com/spinaps/research/sd/?racetrack (last accessed February 2010).